PCCP

Accepted Manuscript

This is an *Accepted Manuscript*, which has been through the Royal Society of Chemistry peer review process and has been accepted for publication.

Accepted Manuscripts are published online shortly after acceptance, before technical editing, formatting and proof reading. Using this free service, authors can make their results available to the community, in citable form, before we publish the edited article. We will replace this *Accepted Manuscript* with the edited and formatted *Advance Article* as soon as it is available.

You can find more information about *Accepted Manuscripts* in the Information for Authors.

Please note that technical editing may introduce minor changes to the text and/or graphics, which may alter content. The journal's standard Terms & Conditions and the Ethical guidelines still apply. In no event shall the Royal Society of Chemistry be held responsible for any errors or omissions in this *Accepted Manuscript* or any consequences arising from the use of any information it contains.

ROYAL SOCIETY OF CHEMISTRY

www.rsc.org/pccp

Viscosity Minima in Binary Mixtures of Ionic Liquids + Molecular Solvents

M. Tariq[1,#], K. Shimizu[2], J. M. S. S. Esperança[1], J. N.Canongia Lopes[1,2,*], L. P. N. Rebelo[1]

[1]Instituto de Tecnologia Química e Biológica António Xavier, Universidade Nova de Lisboa, Av. da República, 2780-157 Oeiras, Portugal

[2]Centro de Química Estrutural, Instituto Superior Técnico, Universidade de Lisboa, 1049-001 Lisboa, Portugal

E-mail: jnlopes@ist.utl.pt

[#]present address: Department of Chemical Engineering, College of Engineering, Qatar University, Doha, 2713, Qatar.

Abstract

The viscosity (η) of four binary mixtures (ionic liquid plus molecular solvent, IL+MS) were measured in the 283.15 < T/K < 363.15 temperature range. Different IL/MS combinations were selected in such a way that the corresponding $\eta(T)$ functions exhibit crossover temperatures at which both pure components present identical viscosity values. Consequently, most of the obtained mixture isotherms, $\eta(x)$, exhibit clear viscosity minima in the studied *T*-*x* range. The results are interpreted using auxiliary Molecular Dynamics (MD) simulation data in order to correlate the observed $\eta(T,x)$ trends with the interactions in each mixture, including the balance between electrostatic forces and hydrogen bonding.

Introduction

The viscosity of pure liquids and liquid mixtures is a complex property and its dependence on temperature and composition poses many demanding challenges in terms of prediction and modeling. This is particularly true for ionic liquids (ILs) and their mixtures with molecular species (MSs).

Pure ionic liquids can exhibit viscosities at room temperature as low as tens of mPa.s or as high as thousands of mPa.s, simply by the replacement of one of its ions (*e.g.* the 1-ethyl-3-methyl imidazolium cation combined either with the dicyanamide or chloride anions). Ionic liquids are also known to be glass-forming materials that can enter supercooled liquid regimes quite easily. This means that their use (and usefulness) as solvation, transport or reaction media will be defined to a great extent by properties such as their solvation dynamics, diffusion coefficients or glass transition temperatures. All these properties are in turn related to the bulk viscosity of the fluid.[1-3]

Around room temperature (and relatively far away from their corresponding glass transition temperatures), the temperature dependence of the viscosity of most ionic liquids, $\eta(T)$, are

Physical Chemistry Chemical Physics Accepted Manuscript

fairly described by the Vogel-Fulcher-Tammann (VFT) equation. Within this framework, ionic liquids —alongside with other glass-forming materials such as polymer-based organic glasses and inorganic glasses— can help to answer some of the fundamental issues related to the nature of the glass transition[4]. One way to proceed would be to study the low-temperature dynamics of ultraviscous ionic liquids.[5]

A different approach is to study IL+MS systems and check the composition dependence of the viscosity of the mixtures[1]. This line of investigation has been explored before in the context of IL+poly(ethylene glycol) mixtures.[6]

Recently, we have shown that commonly employed empirical viscosity mixing rules, which are satisfactorily applicable to MS+MS binary mixtures, yield unreasonable results for many IL+MS systems and their success is highly dependent on the IL:MS viscosity ratio[7]. To further investigate this issue we have selected two molecular solvents, 2-amino-ethanol and 3-amino-1-propanol (2AE and 3AP), both presenting a viscosity/temperature range similar to that of low-viscosity ionic liquids based on 1-alkyl-3-methylimidazolium cations ($[C_n\text{mim}]^+$) combined with dicyanamide ($[\text{DCA}]^-$) or bistriflamide ($[\text{Ntf}_2]^-$) anions. The corresponding binary mixtures exhibit complete liquid-liquid miscibility in the entire composition range and four of them show crossover temperatures where the IL and MS viscosity values are identical (Fig. 1).

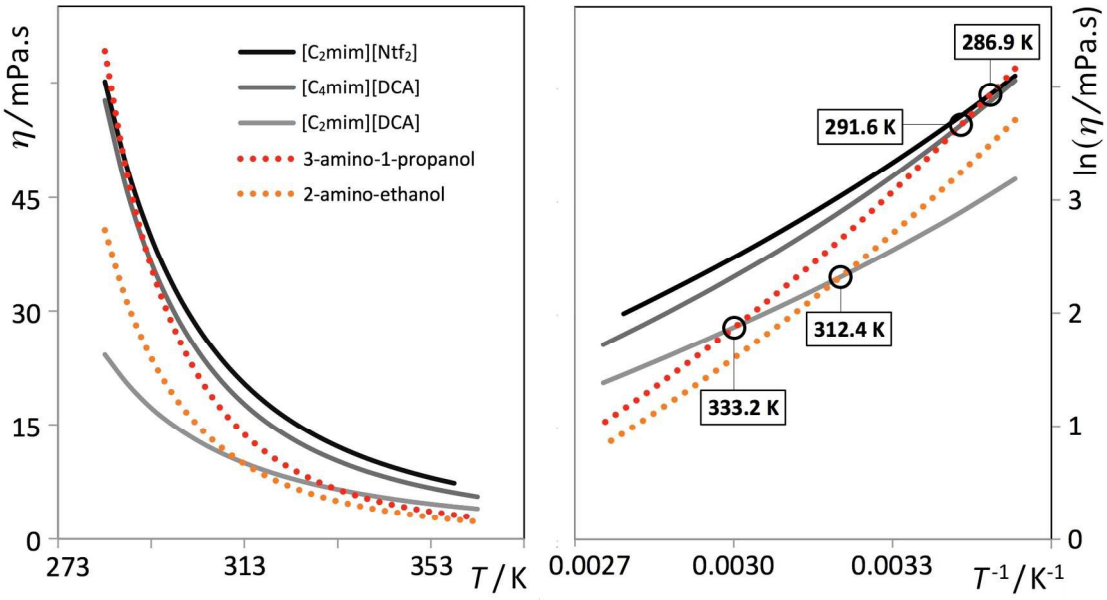

FIG 1. Experimental viscosity data, η/mPa.s, of the three ionic liquids ($[C_2\text{mim}][\text{Ntf}_2]$, $[C_2\text{mim}][\text{DCA}]$ and $[C_4\text{mim}][\text{DCA}]$) and two molecular solvents (2AE and 3AP) studied in this work as a function of temperature. The right-hand plot shows the logarithmic viscosity number as a function of the reciprocal of temperature. The circles indicate the viscosity crossover temperatures.

This state of affairs —the existence of crossover temperatures between the IL and MS components of the binary mixtures— is a consequence of the different cohesive forces and dynamics that characterize the IL or MS systems: the former are dominated by the presence of strong electrostatic forces and the existence of a polar network that permeates the entire liquid and guarantees local electro-neutrality conditions[8]; the latter are governed by strong (-inter

Physical Chemistry Chemical Physics Accepted Manuscript

and –intra) hydrogen bonding between the hydroxyl and amine moieties of the MS molecules[9,10]. The range and temperature-dependence of these forces are quite distinct (Coulomb interactions are long-ranged, isotropic and almost temperature-independent; hydrogen-bonds are contact interactions, directional and highly temperature dependent) and account for the way that the viscosity decreases with increasing temperature in these two classes of compounds: the greater decrease in viscosity versus temperature observed for the two MS compounds can be interpreted as a consequence of the progressive destruction of their hydrogen-bonded intermolecular network as the temperature is increased (cf.Fig. 1). The same discussion could be made in terms of the fragility of the two classes of substance.[11]

What occurs then, when two components with exactly the same viscosity at a given temperature are mixed together? Most empirical viscosity mixing rules (e.g. Grunberg-Nissan rule based on composition-weighted averages of the logarithms of the pure component viscosities[12]) would assume that the viscosity of the ideal mixture should remain unaltered in the entire composition range. Any small positive or negative departure from that situation means that a cross interaction parameter —a measure of the differences between the interactions in the pure components and those in the mixture— must reflect stronger or weaker cross-interactions than the average interactions in the neat compounds. This clear-cut situation is one of the advantages of the present study based on systems showing viscosity crossover temperatures.

The four selected systems also entail the possibility of studying the viscosity departures from the ideal behavior in a systematic way. If the ([C_2mim][DCA] + 3AP) mixture is set as the reference system, then the other three systems represent the effects of changing the anion ([C_2mim][Ntf_2] + 3AP mixture), changing the length of the alkyl side chain in the cation ([C_4mim][DCA] + 3AP mixture), or changing the MS component ([C_2mim][DCA] + 2AE) mixture —cf. Fig.2.

Physical Chemistry Chemical Physics Accepted Manuscript

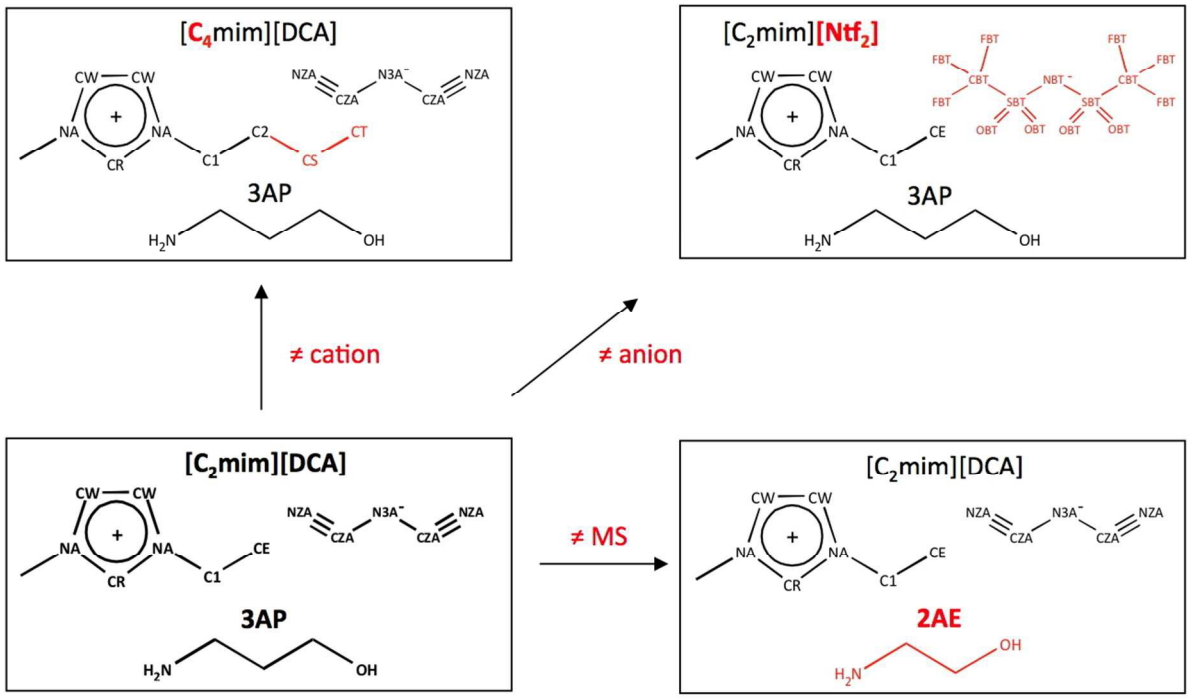

FIG 2. Structural formulas and acronyms of the ionic liquids and molecular solvents contained in the four systems studied in this work. The arrows/red colors indicate the changes operated on the reference system ([C_2mim][DCA]) in order to obtain one of the other three systems.

2. Experimental

2.1. Chemicals

1-ethyl-3-methylimidazolium dicyanamide, 1-butyl-3-methylimidazolium dicyanamide, and 1-ethyl-3-methylimidazolium bistriflamide were purchased from Iolitec (Germany) with stated purity of 99%. 3-amino-1-propanol and 2-amino-ethanol were procured from Sigma Aldrich with stated purity of 99% and 98% respectively. NMR analysis has shown no major impurities in the ILs except traces of water. Before the measurements all IL samples were dried under vacuum and moderate temperature for at least 48 h (beginning at room temperature and gradually increasing up to 333 K over a period of 6 h). The MSs were placed on molecular sieves for a period of one week. Later they were used after filtering to avoid the presence of any dust particles. Prior to mixture preparation the water content of all pure samples were checked using a Karl-Fischer automated titration apparatus and found to be less than 100 ppm, which is adequate for this kind of work.

All mixtures were prepared by weight, just prior to the measurements, in small (5 ml) gas-tight plastic vials using an Ohaus balance with ±0.00001 g precision. The uncertainty in the reported mole fraction is ±0.0001. To ensure proper mixing each vial was tilted upside down several times and stirred in an automated shaker.

Physical Chemistry Chemical Physics Accepted Manuscript

2.2. Viscosity Measurements

The viscosities were measured in the temperature range of 283.15 K to 363.15 K at atmospheric pressure using an automated SVM 3000 rotational Stabinger viscometer-densimeter from Anton Paar. These viscosity measurements are based on a tube filled with the sample in which a hollow measuring rotor floats. Due to its low density, the rotor is centered in the heavier liquid by buoyancy forces. The rotor is forced to rotate by shear stresses in the liquid and is guided axially by a built-in permanent magnet, which interacts with a soft iron ring. The rotating magnetic field delivers a speed signal and induces eddy currents in the surrounding copper casing. These eddy currents are proportional to the speed of the rotor and exert a retarding torque on the rotor. Two different torques influence the speed of the measuring rotor. At equilibrium, the two torques are equal and the viscosity can be traced back to a single speed measurement. The SVM 3000 uses Peltier elements for fast and efficient thermal stability. The temperature uncertainty is ±0.02K from 283.15 to 363.15 K. The precision of the dynamic viscosity measurements is ±0.5%. However, the overall uncertainty of the measurements (taking into account the purity and handling of the samples and the calibration of the Stabinger viscosimeter) is estimated to be 1-2 mPa.s for the present range of viscosities. Further details about the equipment and method can be found elsewhere[13,14].

2.3. Molecular Dynamics Simulations

The CL&P force field[15-17], with parameters specifically tailored to include entire ionic liquid homologous series was used to model all IL ions under consideration. The OPLS-AA force field[18] was used to model the two molecular solvents. All computer simulations were performed using the molecular dynamics package DL_POLY[19].
The force field functional has the general form given in eq. (1)

$$u_{\alpha,\beta} = \sum_{ij}^{\text{bonds}} \frac{k_{ij}}{2}\left(r_{ij} - r_{0,ij}\right)^2 + \sum_{ijk}^{\text{angles}} \frac{\theta_{ij}}{2}\left(\theta_{ijk} - \theta_{0,ijk}\right)^2 + \sum_{ijkl}^{\text{dihedrals}} \sum_{m=1}^{4} \frac{V_{m,ijkl}}{2}\left[1 - (-1)^m \cos\left(m\phi_{ijkl}\right)\right] + \sum_{ij}^{\text{nonbonded}} \left\{ 4\varepsilon_{ij}\left[\left(\frac{\sigma_{ij}}{r_{ij}}\right)^{12} - \left(\frac{\sigma_{ij}}{r_{ij}}\right)^{6}\right] + \frac{1}{4\pi\varepsilon_0}\frac{q_i q_j}{r_{ij}} \right\} \quad (1) \tag{1}$$

with the traditional decomposition of the potential energy, $u_{\alpha\beta}$, into covalent bond stretching, valence angle bending, torsion barriers around dihedral angles, and atom-atom pair-wise repulsive, dispersive, and electrostatic contributions. The Coulomb interactions are defined in terms of fixed atomic point charges while the (12-6) Lennard-Jones potential describes the repulsive and dispersive terms. These non-bonded interactions act either between sites in different molecules or between sites in the same molecule separated by three or more bonds. A scaling factor of 0.5 is applied to the Lennard-Jones and Coulombic interactions when sites in the same molecule are exactly three bonds apart.

Physical Chemistry Chemical Physics Accepted Manuscript

MD simulations were used to study the three different ionic liquids ([C_2mim][DCA], [C_4mim][DCA] and [C_2mim][Ntf_2]), 2-amino-ethanol (2AE), 3-amino-1-propanol (3AP) and their mixtures. For each system studied, we started from low-density initial configurations composed of 200 ion pairs for [C_2mim][DCA] and [C_4mim][DCA], 300 ion pairs for [C_2mim][Ntf_2], 400 molecules of 2AE and 400 molecules of 3AP For the mixtures we used 150 [C_2mim][DCA] ion pairs added to 150 2AE molecules, 180 [C_2mim][DCA] ion pairs with 120 3AP molecules, 120 [C_4mim][DCA] ions pairs plus 180 3AP molecules, and 120 [C_2mim][Ntf_2] ion pairs combined with 180 3AP molecules. The variable number of ion pairs / molecules used in each mixture simulation reflects the need to obtain cubic simulations boxes with approximately the same size (ca. 4.0 nm sides). The boxes were equilibrated in isothermal-isobaric ensemble conditions for 700 ps at 300 K using the Nosé-Hoover thermostat and isotropic barostat with time constants of 0.5 and 2 ps, respectively. Successive simulation runs of 1.5 ns each were used to produce equilibrated systems at the studied temperature until no drift on the average properties of the system could be noticed within statistical uncertainty. The overall simulation run in most cases exceeded 6 ns. Electrostatic interactions were treated using the Ewald summation method considering six reciprocal-space vectors, and repulsive-dispersive interactions were explicitly calculated below a cutoff distance of 1.6 nm (long-range corrections were applied assuming the system has an uniform density beyond that cutoff radius).

Furthermore, in order to estimate the cohesive energy of the liquid phase, simulations were also carried out in the ideal gas phase. In the case of the ILs, it was assumed that such gas phase is composed exclusively by isolated neutral ion pairs, a notion based on experimental evidence for this type of ionic liquids[20,21]. In the case of the MSs, the gas-phase simulations were carried out using isolated 2AE or 3AP molecules. All simulations were performed under micro-canonical ensemble *NVE* conditions for 4 ns. The average temperature during the production runs was similar to that selected for the NPT simulations in the liquid phase (300 K). Electrostatic interactions were treated using the direct coulomb sum method, and repulsive-dispersive interactions were explicitly calculated below a cutoff distance of 50 nm. Since the statistics are poor due to the small number of atoms, each production run took 4 ns and 100 such runs were used to calculate the average gas-phase properties.

3. Results and Discussion

3.1 Experimental Viscosity data: $\eta(T)$ accuracy and $\eta(T,x)$ fitting

All experimental $\eta(T,x)$ data obtained in this work are compiled in Table 1 and depicted in figure 3. Figure 4 shows the experimental data corresponding to the temperature dependence of the viscosity of the five pure components analyzed in this work and compares them with results from other authors. The viscosity data from the present work are consistent with the trends observed for most of the results published for the same systems by other authors (cf. insets of Figure 4). It must be stressed that the observed deviations or uncertainties of 1-2 mPa.s in the determination of the viscosity of the pure components will not affect the results for the mixtures due to error cancellation (cf. discussion below).

Physical Chemistry Chemical Physics Accepted Manuscript

Table 1. Experimental viscosity data, η/mPa.s, of four (ionic liquid plus molecular solvent) binary mixtures as a function of the ionic liquid mole fraction and nominal temperature.

T/K	283	288	293	298	303	308	313	318	323	328	333	338	343	348	353	358	363
x(1)	[C_2mim][DCA] (1) + 3AP (2)																
0.000	64.19	47.47	35.80	27.55	21.51	17.07	13.74	11.20	9.25	7.72	6.51	5.54	4.76	4.12	3.59	3.16	2.79
0.127	44.44	33.78	26.15	20.64	16.54	13.43	11.05	9.21	7.76	6.61	5.69	4.95	4.34	3.83	3.40	3.04	2.73
0.204	36.46	28.15	22.11	17.73	14.40	11.84	9.87	8.31	7.11	6.13	5.34	4.69	4.15	3.70	3.32	2.99	2.71
0.325	28.48	22.47	18.04	14.77	12.25	10.29	8.76	7.54	6.54	5.73	5.06	4.50	4.03	3.64	3.30	3.00	2.75
0.410	25.26	20.27	16.48	13.68	11.46	9.73	8.36	7.26	6.36	5.62	5.00	4.48	4.04	3.67	3.35	3.07	2.82
0.520	22.66	18.46	15.24	12.83	10.91	9.39	8.16	7.15	6.33	5.64	5.06	4.57	4.15	3.78	3.47	3.20	2.96
0.613	21.54	17.74	14.80	12.58	10.79	9.35	8.19	7.23	6.43	5.76	5.19	4.71	4.30	3.94	3.62	3.35	3.11
0.720	21.13	17.58	14.80	12.68	10.96	9.56	8.42	7.47	6.68	6.01	5.44	4.95	4.53	4.17	3.84	3.56	3.31
0.845	21.70	18.20	15.41	13.27	11.53	10.11	8.94	7.96	7.14	6.44	5.84	5.33	4.88	4.50	4.16	3.85	3.59
0.916	22.56	18.94	16.07	13.86	12.05	10.57	9.35	8.33	7.48	6.75	6.13	5.59	5.12	4.72	4.36	4.05	3.77
1.000	24.21	20.30	17.20	14.82	12.88	11.29	9.98	8.88	7.96	7.18	6.52	5.94	5.44	5.00	4.62	4.28	3.98
x(1)	[C_2mim][DCA] (1) + 2AE(2)																
0.000	40.66	30.81	23.78	18.67	14.9	12.04	9.86	8.17	6.85	5.81	4.97	4.29	3.73	3.27	2.88	2.56	2.28
0.108	29.06	22.56	17.8	14.34	11.72	9.68	8.11	6.87	5.88	5.09	4.44	3.9	3.46	3.08	2.76	2.49	2.26
0.205	23.14	18.35	14.76	12.12	10.07	8.47	7.22	6.21	5.40	4.73	4.18	3.72	3.33	3.00	2.72	2.48	2.27
0.300	20.13	16.22	13.26	11.06	9.32	7.95	6.86	5.97	5.25	4.64	4.14	3.72	3.36	3.05	2.78	2.55	2.35
0.407	18.70	15.33	12.71	10.73	9.14	7.87	6.84	6.00	5.30	4.73	4.25	3.84	3.49	3.19	2.93	2.70	2.51
0.500	18.11	14.99	12.53	10.68	9.17	7.95	6.96	6.15	5.47	4.91	4.43	4.03	3.67	3.37	3.11	2.88	2.67
0.613	18.11	15.11	12.74	10.93	9.47	8.28	7.30	6.49	5.81	5.23	4.74	4.32	3.96	3.65	3.37	3.13	2.91
0.739	19.00	15.94	13.53	11.67	10.15	8.91	7.89	7.04	6.32	5.71	5.19	4.74	4.35	4.01	3.71	3.44	3.21
0.813	19.87	16.71	14.2	12.28	10.69	9.39	8.33	7.43	6.68	6.04	5.49	5.01	4.60	4.24	3.93	3.65	3.40
0.903	21.34	17.97	15.27	13.20	11.5	10.11	8.96	8.00	7.18	6.50	5.9	5.39	4.95	4.56	4.22	3.92	3.65
1.000	24.21	20.30	17.20	14.82	12.88	11.29	9.98	8.88	7.96	7.18	6.52	5.94	5.44	5.00	4.62	4.28	3.98
x(1)	[C_4mim][DCA] (1) + 3AP (2)																
0.000	64.19	47.47	35.80	27.55	21.51	17.07	13.74	11.20	9.25	7.72	6.51	5.54	4.76	4.12	3.59	3.16	2.79
0.114	50.89	38.34	29.44	23.01	18.30	14.77	12.09	10.02	8.40	7.12	6.11	5.28	4.61	4.05	3.59	3.20	2.87
0.216	43.35	33.07	25.73	20.43	16.48	13.50	11.21	9.43	8.02	6.89	5.97	5.22	4.60	4.09	3.65	3.28	2.97
0.313	39.67	30.63	24.12	19.38	15.80	13.09	10.98	9.32	8.00	6.93	6.06	5.34	4.74	4.24	3.82	3.46	3.14
0.420	37.88	29.59	23.56	19.12	15.75	13.16	11.14	9.54	8.25	7.20	6.34	5.62	5.02	4.52	4.09	3.72	3.40
0.507	37.77	29.24	23.81	19.46	16.14	13.56	11.54	9.93	8.63	7.56	6.68	5.95	5.33	4.81	4.36	3.98	3.64
0.615	38.96	30.85	24.89	20.45	17.04	14.39	12.30	10.63	9.27	8.15	7.23	6.45	5.80	5.24	4.77	4.35	4.00
0.742	42.21	33.55	27.16	22.38	18.72	15.85	13.58	11.75	10.27	9.04	8.03	7.18	6.46	5.84	5.31	4.86	4.46
0.819	45.35	36.06	29.19	24.04	20.09	17.00	14.56	12.60	11.00	9.70	8.60	7.69	6.91	6.25	5.69	5.20	4.77
0.899	49.66	39.40	31.83	26.15	21.81	18.44	15.77	13.62	11.88	10.46	9.27	8.27	7.43	6.72	6.10	5.57	5.11
1.000	57.65	45.39	36.42	29.75	24.69	20.77	17.68	15.22	13.23	11.6	10.26	9.12	8.18	7.37	6.68	6.09	5.57
x(1)	[C_2mim][Ntf_2] (1)+ 3AP (2)																
0.000	64.19	47.47	35.80	27.55	21.51	17.07	13.74	11.20	9.25	7.72	6.51	5.54	4.76	4.12	3.59	3.16	2.79
0.107	53.40	40.19	30.85	24.13	19.18	15.48	12.67	10.50	8.80	7.44	6.36	5.49	4.77	4.18	3.69	3.28	2.93
0.210	48.18	36.71	28.52	22.58	18.16	14.82	12.26	10.26	8.68	7.43	6.42	5.58	4.89	4.32	3.84	3.44	3.10
0.319	45.45	35.04	27.53	22.04	17.91	14.75	12.31	10.40	8.88	7.65	6.65	5.83	5.16	4.59	4.11	3.70	3.35
0.407	44.15	34.36	27.23	21.98	18.00	14.94	12.56	10.68	9.16	7.92	6.88	6.02	5.33	4.74	4.24	3.84	3.51
0.509	43.99	34.56	27.63	22.49	18.57	15.54	13.17	11.27	9.73	8.47	7.45	6.59	5.87	5.27	4.76	4.32	3.94
0.647	44.25	35.17	28.41	23.36	19.49	16.44	14.05	12.12	10.56	9.28	8.23	7.33	6.58	5.94	5.39	4.92	4.50
0.737	45.80	36.60	29.78	24.60	20.62	17.50	15.02	13.03	11.41	10.07	8.94	7.99	7.17	6.48	5.89	5.38	4.94
0.887	50.73	41.06	33.70	28.05	23.67	20.22	17.47	15.23	13.32	11.80	10.52	9.44	8.51	7.72	7.04	6.44	5.92
1.000	59.51	48.12	39.42	32.77	27.61	23.55	20.27	17.62	15.43	13.61	12.09	10.82	9.71	8.85	8.04	7.34	

Physical Chemistry Chemical Physics Accepted Manuscript

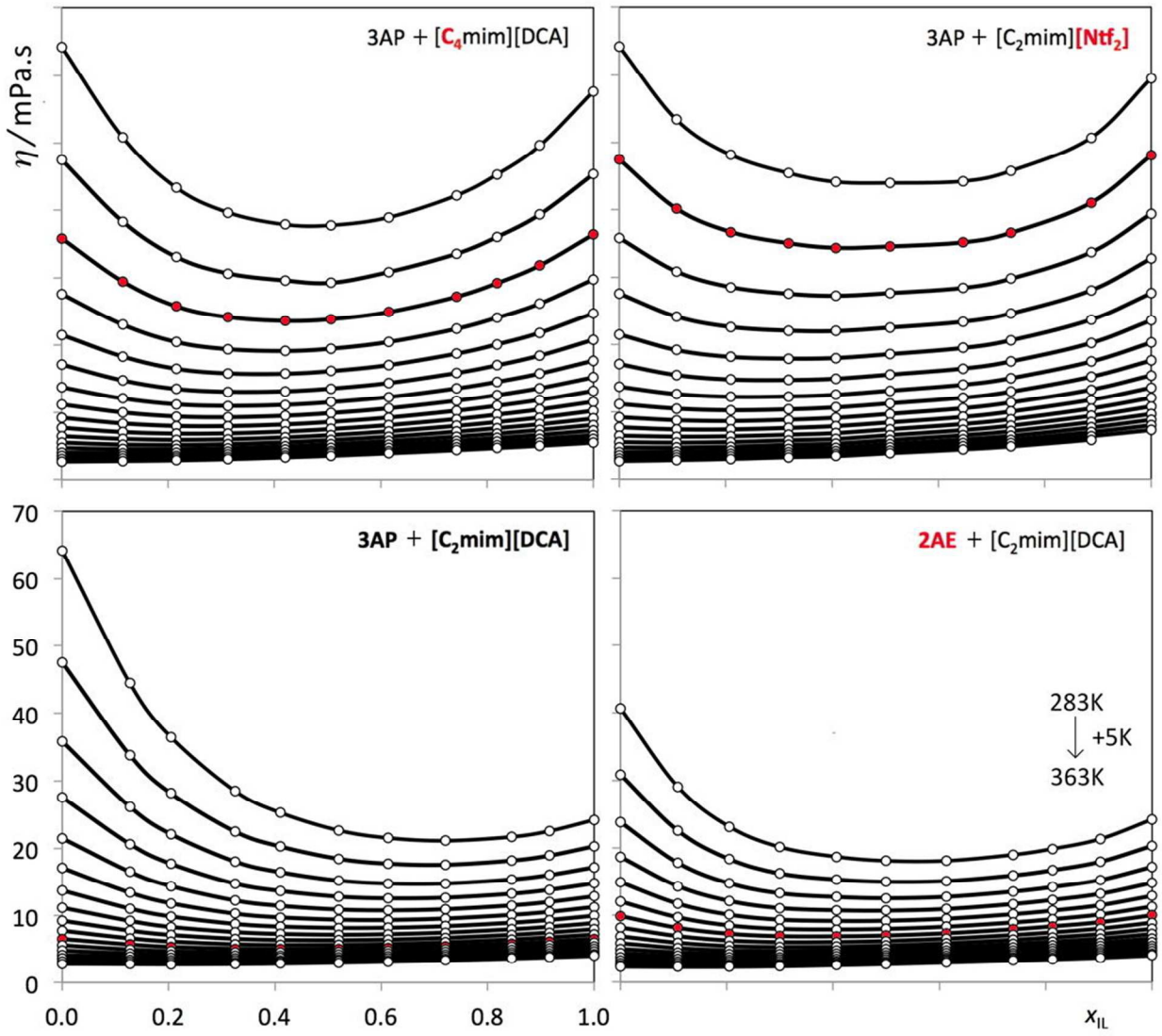

FIG 3. Experimental viscosity data, η/mPa.s, of four (ionic liquid plus molecular solvent) binary mixtures as a function of the ionic liquid mole fraction, x_{IL}. The curves represent different isotherms (cf. inset).The red circles denote for each system the isotherm closest to the viscosity crossover temperature, cf. temperature insets in Fig. 1.

Physical Chemistry Chemical Physics Accepted Manuscript

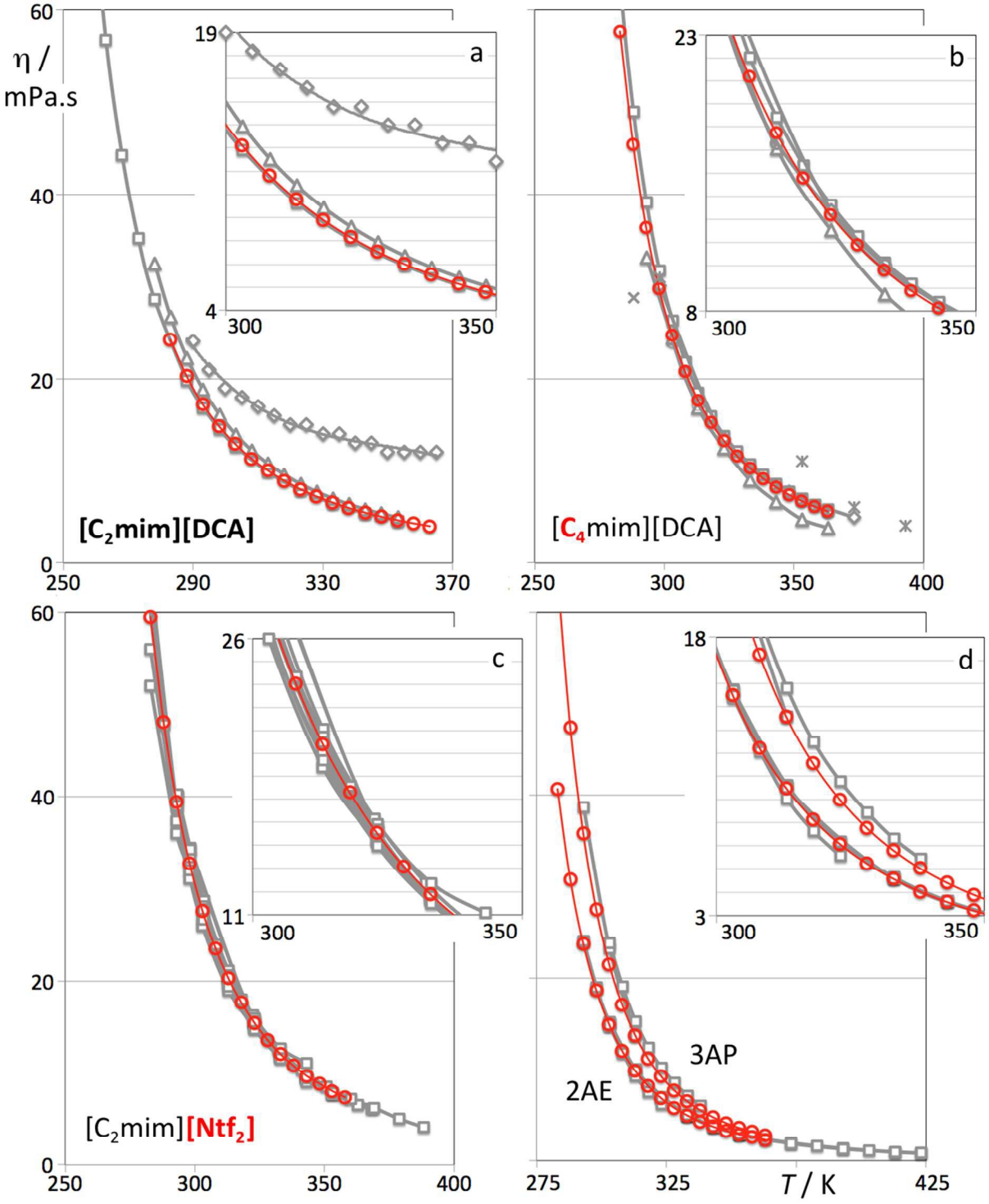

FIG 4. Experimental viscosity data, η/mPa.s, for the three pure ionic liquids (a-c) and two molecular solvents (d) used in this work. This work as red circles/lines. (a) squares: 22, rhombs: 23, triangles: 24; (b) squares: 25-27, triangles: 28, crosses: 29; stars: 30; (c) squares 22,31-38; (d) squares 39-45. The horizontal gridlines in the insets correspond to intervals of 1.25 mPa.s, i.e. close to the estimated uncertainty of the viscosity measurements.

Physical Chemistry Chemical Physics Accepted Manuscript

As shown in Figure 1b, the viscosity data for all studied pure components follow approximately an Arrhenius-type temperature dependence, i.e., the logarithm of the viscosity can be fitted to a second-order polynomial series of the inverse of temperature: $\ln(\eta) = a + b/T + c/T^2$. On the other hand, the composition dependence for a given isotherm of the logarithm of the mixtures viscosity can be expressed as a second-order polynomial of the mole fraction $\ln(\eta) = A + Bx + Cx^2$. Therefore, we have chosen to fit all $\eta(T,x)$ data for a given system to a single surface, eq. (2).

$$\ln(\eta) = (a_A + b_A/T + c_A/T^2) + (a_B + b_B/T + c_B/T^2).x + (a_C + b_C/T + c_C/T^2).x^2 \quad (2)$$

The nine parameters describing such surface for each of the four studied mixtures are given in table 2 and the surfaces themselves, $\ln(\eta(T,x))$, are depicted in Figure 5. The figure also shows for each system the location of the viscosity minimum for each isotherm and the isotherm closest to the viscosity crossover temperature.

Table 2. Fitting parameters (eq.(2)) for the four studied systems. The relative standard deviation of the fit to the experimental $\ln(\eta(T,x))$ data using eq. (2) is 1.33, 0.65, 0.74 and 0.38% for the four listed systems, respectively.

System	a_A	b_A/K	$c_A/10^3K^2$	a_B	b_B/K	$c_B/10^3K^2$	a_C	b_C/K	$c_C/10^3K^2$
$[C_2mim][DCA]$+2AE	2.1052	-3835.6	1249.0	4.0086	316.82	-660.35	-5.0841	1960.3	25.912
$[C_2mim][DCA]$+3AP	1.8512	-3512.4	1137.2	2.3131	1324.5	-771.57	-3.0425	554.55	264.50
$[C_4mim][DCA]$+3AP	2.1346	-3849.5	1249.4	5.6155	-978.26	-333.56	-4.2229	1347.3	112.37
$[C_2mim][Ntf_2]$+3AP	1.7398	-3572.6	1202.9	3.5702	-145.49	-361.58	-2.3909	933.19	39.322

Physical Chemistry Chemical Physics Accepted Manuscript

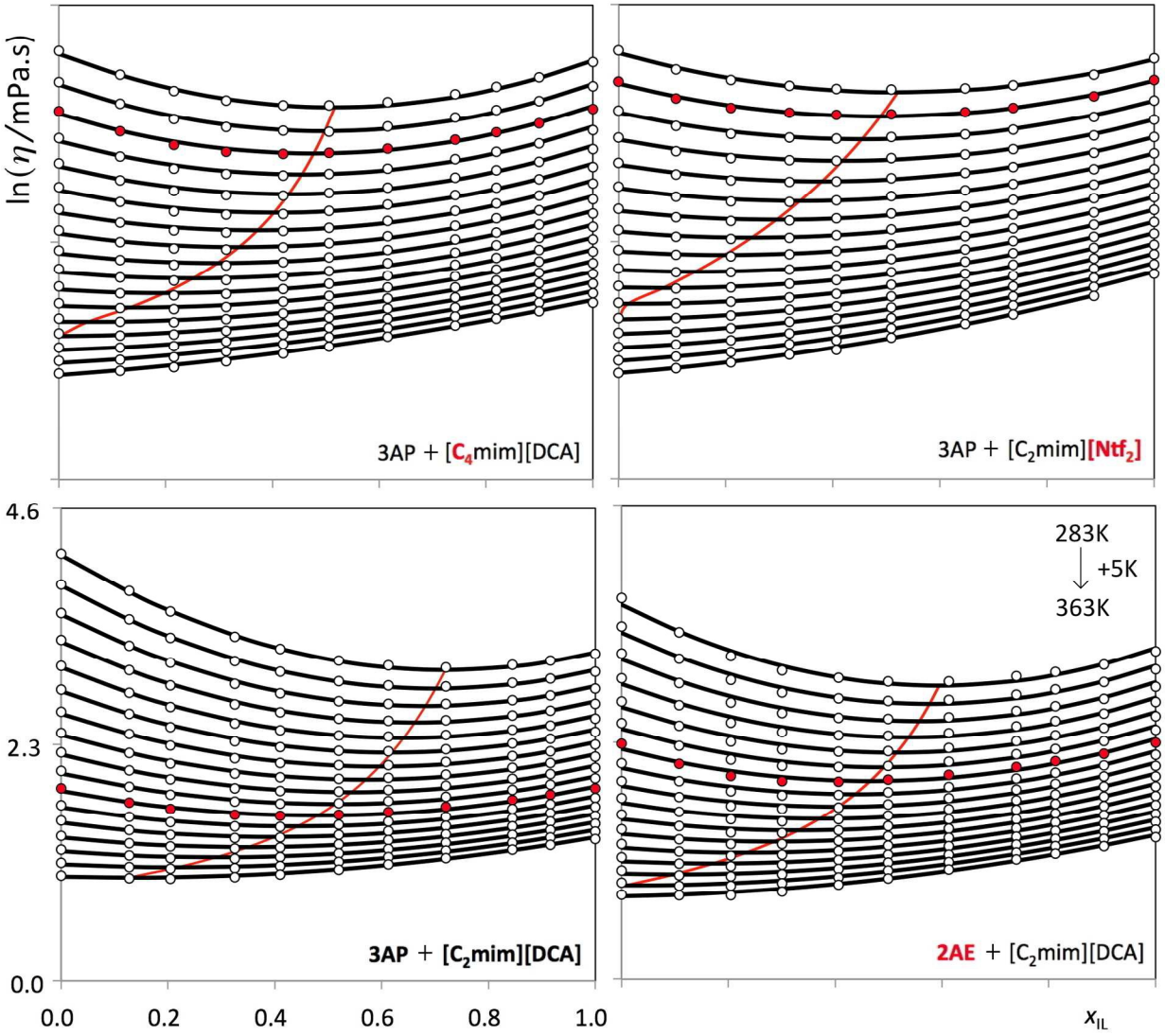

FIG 5. Fitted viscosity data, η/mPa.s, of the four studied mixtures as a function of the ionic liquid mole fraction, represented in a logarithmic scale. The red markers denote for each system the isotherm closest to the viscosity crossover temperature. The red lines are the loci of the mixtures' minima for each isotherm.

3.2 Viscosity data trends: η(*T*) crossovers and η(*T*,*x*) minima

The ln(η(*T*,*x*)) plots expose quite vividly four different issues: i) the points on the left side of each diagram are more spaced than their counterparts on the right side demonstrating the different temperature dependence of the viscosity of the MS and IL components; ii) for the top (lower-temperature) isotherms η(MS)>η(IL) whereas for the bottom (higher temperatures) isotherms the inverse is true, which implies the existence of a crossover temperature in each

Physical Chemistry Chemical Physics Accepted Manuscript

system; iii) most isotherms exhibit a viscosity minimum that is closer to the IL side at the lowest temperatures and shifts to compositions richer in the MS as the temperature increases; iv) at the crossover temperatures most systems exhibit a viscosity minimum close to the equimolar composition (slightly shifted towards MS-rich compositions). The figure shows that although the viscosity ranges at the four crossover temperatures are quite distinct (from 34 <η/mPa.s < 48 for the ([C_2mim][Ntf_2] + 3AP mixture to 5 <η/mPa.s < 6 for the ([C_2mim][DCA] + 3AP mixture), the behavior of the four systems is quite congruent over the entire ln(η(*T*,*x*)) surface, which warrants possible comparisons between them (cf. below).

The existence of the crossover temperatures in the selected system does not constitute in itself any surprise since we have carefully selected the different components in order to achieve such effect —we have combined low-viscosity ILs with high-viscosity MS and used the fact that the viscosities of the later decrease more rapidly with temperature than those of the former (cf. Introduction) to obtain the desired crossovers. What really needs some explanation is the fact that there are pronounced decreases in the viscosity of the mixture when two components with the same viscosity are mixed together: in all cases the viscosity of the equimolar mixtures is 20 to 35% lower than the viscosity of the pure components (8 to 16% lower if logarithms are applied to the viscosity data). Such comparison is depicted in Figure 6 where the relative decrease in the logarithm of viscosity (the departure from the "ideal" behavior given by the Grunberg-Nissan rule) is given for selected isotherms of the four studied systems. The isotherms closer to the crossover temperatures in each case are also depicted. The figure shows that the relative decreases in viscosity, δ ln(η/mPa.s), over the studied temperature range follow the trend ([C_2mim][DCA] + 2AE) > ([C_2mim][DCA] + 3AP) > ([C_4mim][DCA] + 3AP) > ([C_2mim][Ntf_2] + 3AP).

Physical Chemistry Chemical Physics Accepted Manuscript

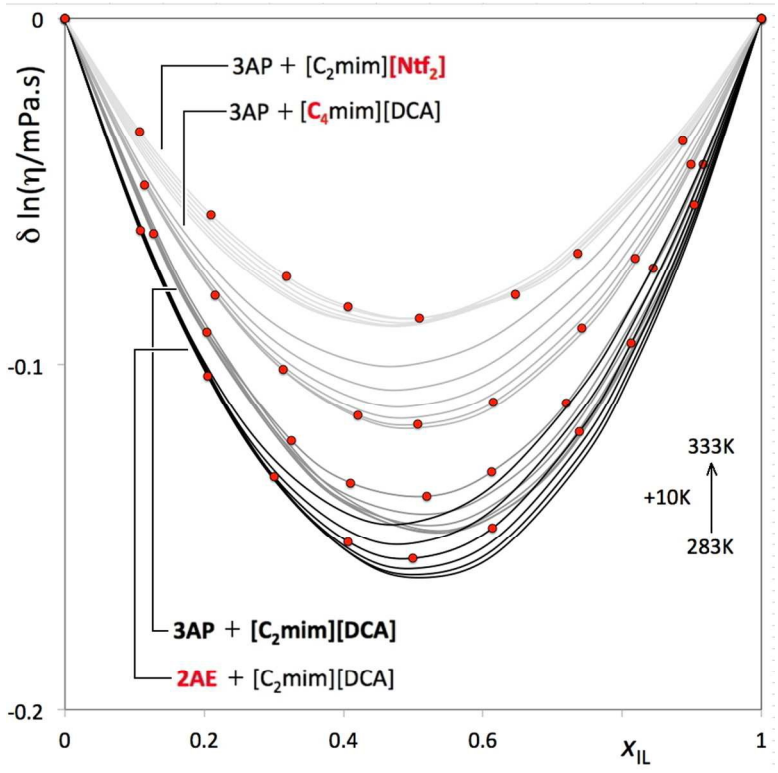

FIG 6. Relative deviations from ideal behavior of the logarithmic viscosity number data, δ ln(η/mPa.s), as a function of the ionic liquid mole fraction. In all cases the graph highlights the quasi-symmetrical behavior around the equimolar composition. The red circles denote for each system the isotherm closest to the viscosity crossover temperature.

3.3 Viscosity and the structure / interactions of complex liquids and their mixtures

At the molecular level the viscosity of a fluid is a measure of the internal fluid friction, which tends to oppose any change in the dynamics of the fluid motion, i.e., viscosity must reflect the effects of molecular/ionic size and motion, structure and interactions. Whereas the mechanism and theory of gas viscosity are reasonably well understood via the application of the kinetic theory of gases and its modifications, the theory of liquid viscosity, especially in the case of complex liquids and their mixtures, is much less developed. In the present case the range of studied viscosities represents the high-end limit for molecular species of comparable molecular weight and the low-end limit for ionic liquids.

As far as molecular interactions are concerned the cohesive energies of the two classes of components (MS versus ILs), as attested by the corresponding vaporization enthalpies at room temperature, are quite distinct: 2AE and 3AP exhibit values of 60 and 70 kJ/mol[46,47], respectively, whereas typical ILs exhibit values above 135 kJ/mol[48]. In the case of the two studied MSs a large proportion of the cohesive energy stems from hydrogen bonding between the hydroxyl and amino groups in the molecules: the two alkanes with similar molecular weight

Physical Chemistry Chemical Physics Accepted Manuscript

/ dimensions to 2AE and 3AP —*n*-butane and *n*-pentane— exhibit vaporization enthalpies ca. 40 kJ/mol lower than the corresponding amino-alkanol molecules. Those 40 kJ/mol (quite close to the value for the enthalpy of vaporization of water) can be understood as the energy necessary to break the hydrogen bonds between the two proton acceptor/donor centers in the 2AE or 3AP molecules. On the other hand, in the case of ILs, MD simulations[21,49] have shown that electrostatics play an important role (contributing with more than 50% in some cases) in the description of the cohesive energy of the liquid. Interactions between specific sites in the cation and in the anion (sometimes also dubbed as (proto-)hydrogen bonds) can also have significant contributions to the total cohesive energy. In summary, even if at some temperature the two classes of compounds exhibit viscosity crossovers, both the nature and magnitude of their cohesive energies remain quite distinct. In other words, although more intense intermolecular interactions generally lead to more viscous flows in a liquid, other factors such as the anisotropy of the forces, the shape of the molecules and the supramolecular structure of the fluid play an important role in the definition of the viscosity of the liquid media.
For instance, the condensed phase of ILs should not be regarded as just a collection of ion pairs (in an ionic fluid each cation is surrounded by a first shell of several anions and vice-versa), which means that in order to move within the liquid the ions do not have to overcome energy barriers as those indicated by the corresponding vaporization enthalpies —ions are able to diffuse while keeping some of their first-contact neighbors and maintaining always a sizeable proportion of their overall electrostatic interactions. On the other hand in the case of hydrogen-bonded molecular species, the movement of the molecules implies the rupture/ restoration of the highly directional H-bonds intermolecular interactions, which can denote sizeable energy barriers in those cases where the process cannot be accomplished in a concerted manner.

3.4 Molecular Dynamics simulations: overall structure, energetics and auto-diffusion

In order to explore more effectively the relation between structure, interactions and viscosity in the studied systems, we have performed a series of Molecular Dynamics simulations where we have modeled all components in a consistent manner using a fixed-charge atomistic force field (cf. MD Simulations Section). It must be stressed at this stage that it is known that such force field does not yield the correct viscosity values (they are generally overestimated by more than one order of magnitude). This is a consequence of the non-polarizable nature of the force field that overemphasizes the intensity of the electrostatic interactions between ionic species. This issue can be corrected by one of several charge-transfer/re-parameterization schemes[50,51] that can improve significantly the dynamics and energetics of the simulation. However it is also known that in most of those schemes the price to pay for the reduction of the effective point charges in the interaction centers of the ionic species is a poorer description of possible hydrogen bonds between some of those centers[52]. Since we want to focus our discussion in the interplay between electrostatic and hydrogen-bonds and we will extend the simulations to mixtures of ILs and MSs (where the implementation of a charge-transfer scheme may cause some consistency problems in the case of the neutral molecules) we have decided to keep the original force field and center our analysis on the differences between the structure and energetics of the pure components and their mixtures, the calculation of specific interactions

Physical Chemistry Chemical Physics Accepted Manuscript

(hydrogen-bond type interactions) between species and how these may influence the experimentally observed viscosity trends. Given the inadequacy of the used force field we will not estimate the viscosity of the simulated systems. In our opinion this should be attempted only when a polarizable force field becomes available for ILs and their mixtures with molecular species.

Nevertheless, from a qualitative point of view, the self-diffusion coefficients of the different species (obtained from the mean square displacement of selected atoms on the corresponding IL ions or MS molecules) yield values at 298 K for the pure components that are consistent with the experimental viscosity data: *e.g.* $D_{C2mim@[C2mim][DCA]} > D_{C4mim@[C4mim][DCA]} > D_{C2mim@[C2mim][Ntf2]}$ implies that $\eta_{[C2mim][DCA]} < \eta_{[C4mim][DCA]} < \eta_{[C2mim][Ntf2]}$ or $D_{2AE} > D_{3AP}$ implies that $\eta_{2AEA} < \eta_{3AP}$. Also, the self-diffusion coefficients of the different species in the mixtures show that the ions tend to diffuse more in the mixture than in the neat IL, whereas the MS species diffuse less relative to the pure MSs. The overall decrease in viscosity is the result of a trade-off between these two opposing trends.

Table 3 summarizes the first set of simulation results where we have calculated the molar density and vaporization enthalpies of the five pure components (three ILs, two MSs) and compared them with the corresponding experimental values at 298 K.

Table 3. MD simulation data and comparison with experimental results.

System Pure	#IL Ion pairs	#MS Molecules	V_{box} nm^3	l_{box} nm	ρ_{sim} mol/dm^3	ρ_{exp}[a] mol/dm^3	ΔH_{sim} kJ/mol	ΔH_{exp}[b] kJ/mol
[C_2mim][DCA]	200	0	53.5	3.77	6.208	6.222	181.5	156
[C_4mim]DCA]	200	0	64.4	4.01	5.159	5.159	182.7	157
[C_2mim][Ntf_2]	300	0	130.2	5.07	3.825	3.866	162.9	138
2AE	0	400	40.3	3.43	16.467	16.568	56.7	60
3AP	0	400	49.8	3.68	13.329	13.090	71.0	70
Mixtures						V^E/Vid %		$\Delta H^E/\Delta H_{id}$ %
[C_2mim][DCA]+2AE[c]	150	150	54.6	3.79	9.124	-1.2	122.2	2.7
[C_2mim][DCA]+3AP[c]	150	150	58.1	3.87	8.577	-1.2	130.8	3.6
[C_2mim][DCA]+3AP[d]	180	120	62.5	3.97	7.969	-0.9	141.5	3.1
[C_4mim][DCA]+3AP[c]	150	150	66.4	4.05	7.504	-0.9	162.9	28.4
[C_4mim][DCA]+3AP[e]	120	180	60.4	3.92	8.243	-1.0	145.2	25.5
[C_2mim][Ntf_2]+3AP[c]	150	150	80.0	4.31	6.224	-4.5	141.0	20.5
[C_2mim][Ntf_2]+3AP[e]	120	180	71.3	4.15	6.990	-4.4	127.6	18.4

[a][44,45,53,54]; [b][46 - 48,55];[c]equimolar; [d]$x_{IL} = 0.6$; [e]$x_{IL} = 0.4$

The liquid densities of most pure components are estimated within 2% uncertainty.[44,45,53,54] These uncertainties are consistent with previous results obtained using the present force field and are reasonable and justified by the underlying generality and transferability of the model.
In the case of the ILs, the stronger electrostatics introduced by the use of the original fixed-charge force field model cause the overestimation of the simulated ΔH_{vap} values by ca. 25 kJ/mol relative to the corresponding experimental values (135-141 kJ/mol and 157 kJ/mol for [C_2mim][Ntf_2] and [C_4mim][DCA], respectively[48,55]). There are no experimental values reported

Physical Chemistry Chemical Physics Accepted Manuscript

for [C_2mim][DCA] but it is probable that the estimated value is also over-predicting the real value by approximately the same amount. In the case of the two amino-alkanols, the estimated values lie much closer (less than 4 kJ/mol) to the experimental ones (60 and 70kJ/mol for 2AE and 3AP, respectively[46,47].

The density and vaporization enthalpy results indicate that the force field is able to model adequately the components of the mixtures (taking into account the caveats mentioned at the beginning of this section) so the next step is to check what happens to the density and cohesive energy of the system when mixtures of (IL+MS) are considered. Seven mixtures were simulated: four equimolar mixtures of the four systems considered in this study plus three extra mixtures for those systems where the viscosity minima of the 298 K isotherm do not lie near the equimolar composition (cf. Figure 5, Table 3).

The results show that in all cases the molar volume of each mixture is smaller than the composition-weighted average of the molar volumes of the pure components (the "ideal" molar volumes). All mixtures contract by about 1% relative to the ideal volume of the mixture, except for the case of the ([C_2mim][Ntf_2] + 3AP) mixtures that contract around 4.5%. The simulations also show that the cohesive energy of the mixtures is larger than the composition-weighted average of the cohesive energies of the pure components. In this case the fluids become more cohesive by around 3% for the ([C_2mim][DCA] + 2AE) and ([C_2mim][DCA] + 3AP) systems, by ca. 26 % for the ([C_4mim][DCA] + 3AP) mixtures and by around 20% for the ([C_2mim][Ntf_2] + 3AP) system.

These trends seem counter-intuitive since we have seen that all mixtures exhibit lower viscosities than the corresponding composition-weighted average of the pure components. However, one should be wary to note that there is no simple relation between larger densities or cohesive energies and higher viscosities: after all the two pure components can have in some cases the same viscosity but exhibit always completely different densities and cohesive energy values. The important point to note is that the simulations show that the ([C_2mim][DCA] + 2AE) and ([C_2mim][DCA] + 3AP) show quasi-ideal behavior whereas the ([C_4mim][DCA] + 3AP) and ([C_2mim][Ntf_2] + 3AP) show larger deviations from that behavior(larger densities and/or cohesive energies). This supports the experimental results that show smaller viscosity drops in the two later mixtures than in the two former ones.

3.5 MD simulations: pair interactions, correlation functions and aggregate analyses

This can be further analyzed if one recognizes that the different behavior of the four systems in terms of their cohesive energy must reflect what is occuring in terms of interactions between the IL and MS species in the mixture. As we have seen hydrogen bonding plays a dominant role in the definition of the cohesive energy of the two selected amino-alkanol MSs and that in the case of imidazolium-based ILs, it can also have an important contribution via the interactions between the more electronegative atoms in the anion (OBT, NZT) and the most acidic hydrogen atoms attached to the imidazolium ring (HCW, HCR), cf. Figure 2. In the IL + MS mixtures it is expected that there will be the formation of new H-bonds between the ions and the molecules, at the expense of the H-bonds that existed in the pure components.

The next set of results to be extracted from the MD simulations is based on clustering analyses involving hydrogen-bonding counting. To tally the number of hydrogen bonds present during

Physical Chemistry Chemical Physics Accepted Manuscript

the simulations, the distances between all hydrogen atoms (acidic Hs) and all possible proton acceptors (electronegative X atoms) for all configurations obtained during the simulation runs were computed and those distances that were lower than a given threshold limit for a given (H-X) pair were considered to be a hydrogen bond (contact) of that given type. The threshold distances were estimated considering the pair radial distribution functions, $g(r)$ or RDFs, between the different possible (H-X) pairs: the first peaks in the corresponding RDFs were fitted to Gaussian curves and their base lines used to define the corresponding distance (cf. Figs. 7 and 8). In the case of hydrogen bonding involving the hydrogen atoms of the MS components the threshold limit was set to 0.26 nm, whereas for those involving the acidic hydrogen atoms of the imidazolium ring the distance was set to 0.31 nm. The difference lies in the fact that the former hydrogen atoms are modeled without a repulsive Lennard-Jones term (σ_{LJ} = 0 pm), while the latter ones have a value of σ_{LJ} = 242 pm).

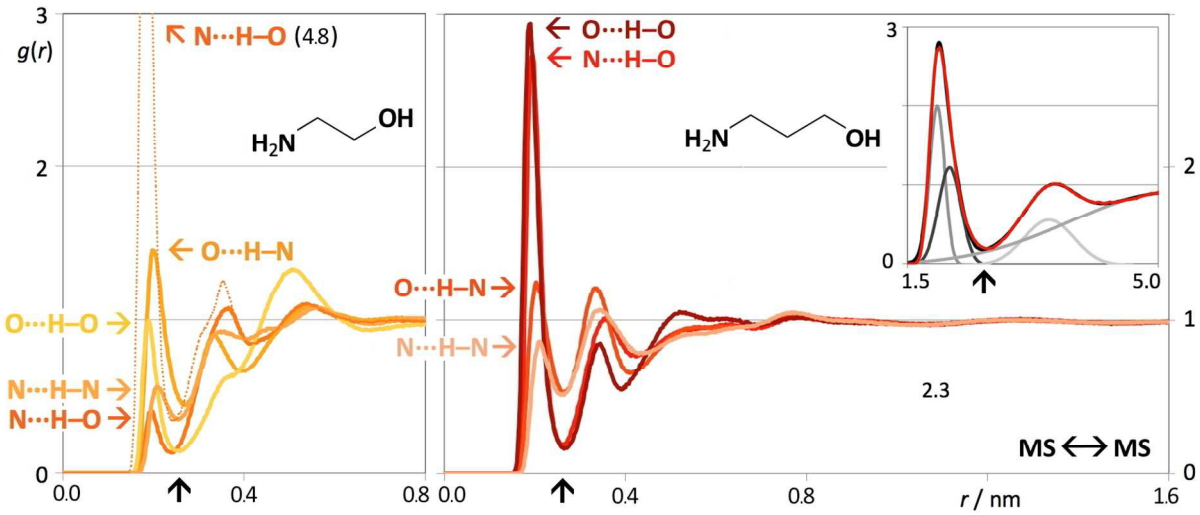

FIG 7. Radial distribution functions between selected pairs of interaction centers (cf. inset molecular structures) in the pure molecular solvents. The arrows indicate the position of the threshold limits used in the hydrogen-bond aggregate analyses. The inset exemplifies the multipeak analysis (Gaussian fitting) used to define such positions for the case of the **N**···**H**–O pair interaction.

Physical Chemistry Chemical Physics Accepted Manuscript

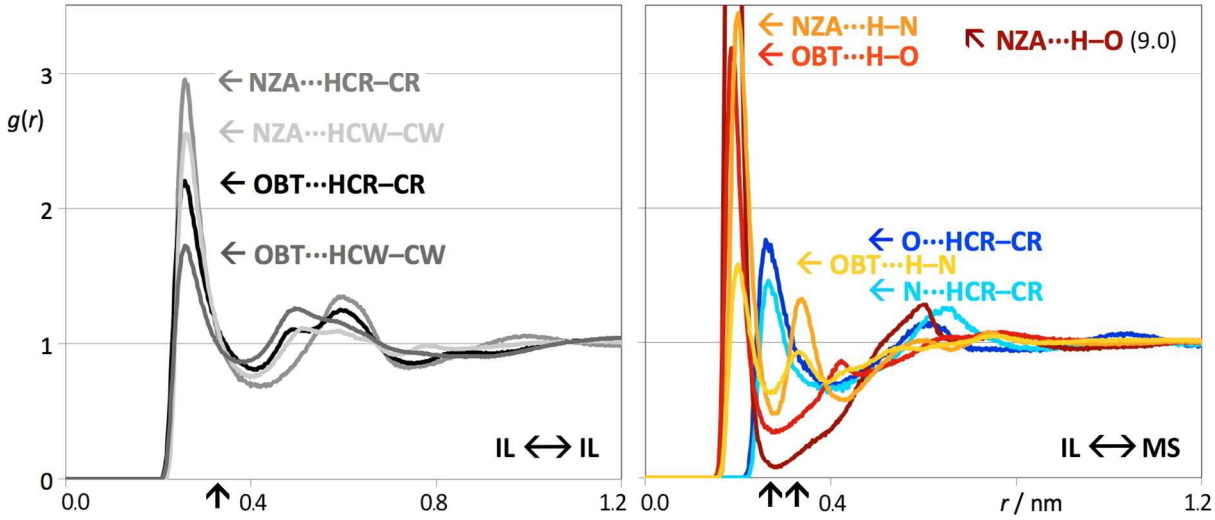

FIG 8. Radial distribution functions between selected pairs of interaction centers in: (left) pure [C_2mim][DCA] and [C_2mim][Ntf_2] (cf. atom designations in Fig. 2); (right) the (IL + MS) mixtures. Arrows as identified in Fig. 7.

The inspection of Figure 7 (RDFs depicting hydrogen bonding in the MSs) point to some interesting and striking differences between the two aminoalkanol molecules. In these molecules there are two types of acidic hydrogen (those directly attached to the nitrogen and oxygen atoms of the hydroxyl and amino groups) and two electronegative atoms with lone pairs of electrons capable of accepting a proton and establish a hydrogen bond (the nitrogen and oxygen atoms). This means that there are four possible combinations in which an hydrogen bond can occur between two aminoalkanol molecules and those will occur at the distances corresponding to the first peaks of the RDFs represented by the filled curves in Figure 7a (2AE) and 7b (3AP). One can immediately notice that the intensity and order of the different combinations is completely different in 2AE (lower intensities, dominance of O···H–N bonds) and 3AP (higher intensities, dominance of O···H–O and N···H–O bonds). This contrasting situation given by the present model can be reconciled if one notices that both molecules can also establish intramolecular H-bonds. In fact it is known that in the diluted gas phase a large proportion of the isolated molecules adopt gauche conformations of the amino and hydroxyl groups allowing for the formation of such intramolecular bonds[56]. In the liquid phase the OPLS model predicts that in the case of the 2AE those intramolecular bonds, namely of the N···H–O type, still persist and constitute a majority whereas for 3AP they are almost absent. This can be seen by adding the intramolecular N···H–O RDF to the previously calculated intermolecular N···H–O RDF (dotted curve of figure 7a). The existence of such intramolecular bonds also explains the relative intensity of the other intermolecular peaks. However, it must be stressed at this point that previous simulation studies involving 2AE showed that the prediction of the relative importance of the intra- and inter-molecular hydrogen bonds in these molecules seem to be very sensitive to the chosen force field and that in the lack of supporting experimental data, they cannot be used as the only criterion in the validation of a given model[57]. In the case of 2AP, Raman studies have shown that in the liquid phase there is a dominance of

Physical Chemistry Chemical Physics Accepted Manuscript

intermolecular H-bonds, which means that the OPLS model (in spite of providing correct ΔH_{vap} and density estimates for 2AP) would have to be modified in order to yield the correct hydrogen bonding relations.

Since it is also difficult to establish a possible and direct relation between molecular mobility / viscosity and the presence of intramolecular interactions, we have decided to exclude the ([C_2mim][DCA] + 2AE) mixture from the rest of the H-bond analyses and include only the 3AP mixtures where, according to the adopted model, intramolecular bonding does not play a leading role. Accordingly, hydrogen bonding data for the other four pure components (three ILs plus 3AP) and six simulated mixtures are given in table 4.

Table 4. Number of contacts (hydrogen bonds) between selected pairs of atoms in the simulated pure components and mixtures. All numbers refer to 1000 MS molecules and/or IL ion pairs in the pure component/mixtures. The Δ values refer to the net gain/loss of number of contacts between the mixtures and the corresponding pure components.

NC types	MS-MS				IL-IL		MS-IL			tot(Δ)
	N···HO	O···HN	O···HO	N···HN	$H_{CR}\cdots X_{ANI}$	$H_{CW}\cdots X_{ANI}$	N···H_{CAT}	O···H_{CAT}	X_{ANI}···HO	
Pure components										
[C_2mim][DCA]					1195	2160				3355
[C_4mim]DCA]					1145	1985				3130
[C_2mim][Ntf_2]					1110	1830				2940
3AP	460	710	490	513						2173
Mixtures										
[C_2mim][DCA]+3AP[a]	30	93	57	73	413	700	317	357	377	2417 (-347)
[C_2mim][DCA]+3AP[b]	30	60	17	43	543	970	240	313	330	2547 (-335)
[C_4mim][DCA]+3AP[a]	33	103	27	77	397	663	283	330	397	2310 (-341)
[C_4mim][DCA]+3AP[c]	63	150	73	133	263	483	280	350	410	2207 (-349)
[C_2mim][Ntf_2]+3AP[a]	77	87	103	77	483	737	270	320	267	2420 (-136)
[C_2mim][Ntf_2]+3AP[c]	167	183	167	120	353	563	280	280	233	2347 (-133)

[a]equimolar; [b]x_{IL} = 0.6; [c]x_{IL} = 0.4

3.6 MD simulations: viscosity and H-bonding trade-offs

The table shows that around 71-93% of the hydrogen bonds present in the pure 3AP are lost when the molecules are incorporated in the studied mixtures (the percentage varies taking into account the nature of the IL and the composition). The same applies to around 55-76% of the specific interactions (hydrogen-bond type) present in the pure ILs. It must be stressed that due to the larger molar volume of the three ILs (161, 186 and 260 cm^3/mol for [C_2mim][DCA], [C_4mim][DCA] and [C_2mim][Ntf_2], respectively) relative to 3AP (76 cm^3/mol), the 40 to 60% mole fraction compositions correspond to mixture volume fractions richer in IL, ranging from 68 to 77% x_V(IL). This means that the loss of MS-MS interactions will always be larger relative to the loss of IL-IL interactions due to the asymmetrical mutual mixing of both components. Those losses are partially compensated by the formation of hydrogen-bonds between the IL ions and the MS molecules (790 to 1050 new specific cross interactions per 1000 molecules/ion pairs of mixture). Finally, the results indicate that in terms of hydrogen-bonding there is a net loss of hydrogen bonds in the mixtures relative to the pure components, ranging from 5 to 13%. It is

Physical Chemistry Chemical Physics Accepted Manuscript

important to stress the relative and semi-quantitative character of the comparisons just carried out based on number of H-bond-like contacts. It is obvious that not all H-bonds have the same intensity or will cause the same net effect on the mobility of a given molecule or ion. However we are always comparing the same type of interactions between the three systems under discussion which means that a relative increase or loss of a given number of contacts must have a consistent impact in terms of the expected overall properties like the viscosity or cohesive energy of the system.

The most conspicuous result is that of the mixture containing $[C_2mim][Ntf_2]$, where the smaller proportions of hydrogen-bond net losses 5% are found. This is consistent with the larger excess density and excessive cohesive energy results (cf. Table 3) and also with the smaller drops in viscosity observed for this system (cf. Fig 5). It is interesting to note that the relatively small H-bond net losses for the $[C_2mim][Ntf_2]$ mixtures are mainly due to smaller losses in the IL-IL interactions relative to the other two systems.

In the case of the ($[C_4mim][DCA]$ + 3AP) system the simulation results yielded hydrogen-bond losses (13%) similar to those observed for the ($[C_2mim][DCA]$ + 3AP) system. However, the relative drop in viscosity in the former system is more modest than in the latter. The difference between the two systems is just the length of the alkyl side chain of the cation, which means that the underlying cause for the viscosity difference may lie in some structural difference caused by such fact.

3.7 MD simulations: IL polar networks and non-polar domains

It is known that ionic liquids are highly structured liquids, composed of a polar network (formed by the charged parts of the ions) surrounded and permeated by non-polar regions (constituted by the alkyl side chains of the cations).[58,59] Those non-polar regions form small clusters ("islands") embedded in the polar network or —if the alky chains are long enough— can even form a domain that percolates and is bi-continuous with the polar network. The highly complex structure of ionic liquids can be analyzed using the trajectories of MD simulations. Figure 9 shows MD simulation snapshots of four configurations representing the pure $[C_2mim][DCA]$ and $[C_4mim][DCA]$ ILs and their two equimolar mixtures with 3AP, along with four radial distribution functions representing the structuration of the polar network in each case.

Physical Chemistry Chemical Physics Accepted Manuscript

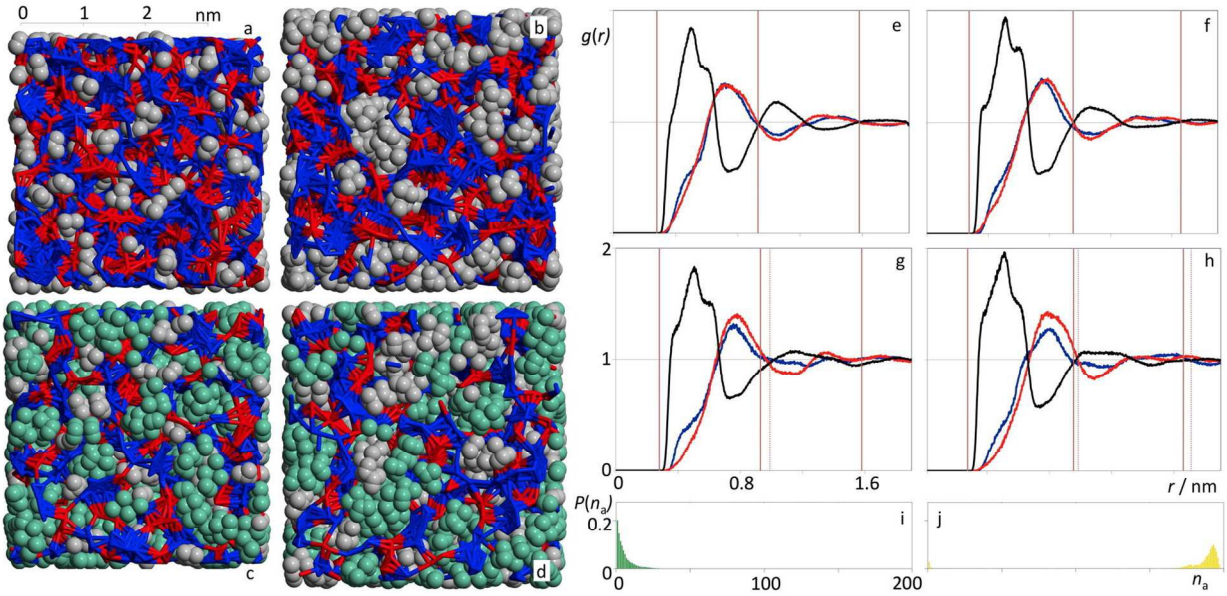

FIG 9. MD snapshots for four studied binary mixtures: (a) pure [C_2mim][DCA]; (b) pure [C_4mim][DCA]; (c) binary mixture of [C_2mim][DCA] with 3AP; (d) binary mixture of [C_4mim][DCA] with 3AP. Pair radial distribution functions, RDFs, between selected pairs of interaction centers belong to charged parts of the ionic liquids: (e) pure [C_2mim][DCA]; (f) pure [C_4mim][DCA]; (g) binary mixture of [C_2mim][DCA] with 3AP; (h) binary mixture of [C_4mim][DCA] with 3AP. Black line: cation-anion RDF between the central atom of the anion (NBT or N3A) and the center of mass of the imidazolium cation (CM); Red line: anion-anion RDF (NBT-NBT or N3A-N3A); Blue line: cation-cation RDF (CM-CM). (i, j) Discrete probability distribution of nonpolar aggregate sizes, $P(n_a)$, as a function of aggregate size number, n_a for [C_2mim][DCA] (green) and [C_4mim][DCA] (yellow).

One of the most conspicuous features of the RDFs representing the cation-anion, cation-cation and anion-anion correlations in an ionic liquid or molten salt is the opposition-of-phase nature between the former (cation-anion) correlation and the (cation-cation and anion-anion) correlations. This is in stark contrast with the correlation functions between the molecules of a liquid formed by neutral molecules where after the few peaks/valleys corresponding to the first neighbor shells of a given atom/interaction center, all RDFs loose rapidly all periodic features (cf. for instance the RDFs of 3AP depicted in figure 7b). Figures 9e and 9f show that both [C_2mim][DCA] and [C_4mim][DCA] have well defined polar network structures, where a given ion is surrounded by successive shells of counter-ions and ions-of-the-same-charge and that such spatial order is still noticeable several shells removed (a few nanometers) from the original ion. The two grids superimposed in the two figures over the nodes of the oscillatory behavior of the RDFs represent the periodicity of such spatial order and their spacing can be directly correlated via the appropriate Fourier-transform to the so-called intermediate q-peaks of the structure-factor spectra of the ionic liquids[59]. When the MS molecules are added to the mixture they do not disrupt the polar network locally (the position and height of the first peaks in figures 9g and 9h is kept) but one notices that i) the nodes are pushed to slightly larger values (the polar network is “stretched”, cf. dotted gridlines in the corresponding figures) and ii) the opposition-of-phase behavior between the RDFs starts to break down soon after the completion of the first period. Apparently such stretching is larger and the breakdown occurs earlier for [C_2mim][DCA]

Physical Chemistry Chemical Physics Accepted Manuscript

than for [C_4mim][DCA]. This state of affairs is consistent with the larger drops in viscosity that occur in the [C_2mim][DCA] mixtures relative to those in the [C_4mim][DCA] ones. The slightly better resilience to de-structuration of the [C_4mim][DCA] system can in turn be related to the presence of larger non-polar clusters in the midst of the polar network: adding the neutral molecules will swell those aggregates but since they have always been present and anchored to the polar network, the latter can cope more effectively with such perturbation; in the case of [C_2mim][DCA] the MS molecules will impinge themselves directly on the "bare and unprepared" polar network. Figure 9 shows the differences between the non-polar domains of the two ionic liquids via the depiction of the corresponding CT-CT RDFs. Aggregate analyses conducted on the size and number of neighbors of such domains are also shown in the figure and indicate that while the alkyl side chains of [C_2mim][DCA] remain in the form of small clusters in the midst of the polar network (>20% as isolated chains, >15% as clusters with just two chains), those of [C_4mim][DCA] form much larger clusters that almost percolate it (the largest probability is to find aggregates that comprise almost all tails contained in the simulation box). Further aggregation analyses have shown that whereas the number of average contact neighbors of a given alkyl side chain is just 1.3 in the case of [C_2mim][DCA], the number is 3.3 for [C_4mim][DCA].

These facts explain not only the higher viscosity of pure [C_4mim][DCA] relative to pure [C_2mim][DCA] (the movements of the ions within the polar network are restricted by the presence of larger non-polar domains) but also the lower drops in the viscosity of the mixtures of [C_4mim][DCA] with 3AP —the addition of 3AP is done on a system that already structured its polar network around a series of non-polar intrusions.

Finally, these structure-based inferences can also be tested for the [C_2mim][Ntf_2] systems. This ionic liquid shows the highest viscosity and the corresponding ionic correlation RDFs depicted in figure 4a of reference 59 show a level of structuration even higher than that observed for [C_2mim][DCA] or [C_4mim][DCA], with an average number of closest neighbors for a given tail of just 0.78 and a probability of finding isolated chains larger than 40%.[59] This would mean that the addition of the MS molecules would cause a large disruption of the polar network and, like in the case of [C_2mim][DCA], relatively large drops in the viscosity of the mixtures. However, there are significant differences between [C_2mim][DCA] and [C_2mim][Ntf_2], namely both the size and flexibility of the anion and its impact in the polar network. This can be observed in the case of [C_{10}mim][Ntf_2], where the existence of very large alkyl side chains does not hinder the existence of an extended periodicity in the spatial ordering of the polar network (unlike the case of $[DCA]^-$-based ILs, $[Ntf_2]^-$-based ILs show distinctive intermediate q-peaks in their structure-factor spectra, even for [C_{10}mim][Ntf_2])[59]. Figure 10 illustrates two snapshots showing the pure [C_2mim][Ntf_2] IL and the corresponding equimolar mixture with 3AP. The swelling of the polar network and the intrusion of the MS in its midst is obvious; however, unlike the case of the $[DCA]^-$-based ILs, the polar network remains much more interconnected. This is in excellent agreement with the H-bond aggregation analyses that showed that there are indeed more modest losses in the IL-IL interactions relative to the other two systems.

Physical Chemistry Chemical Physics Accepted Manuscript

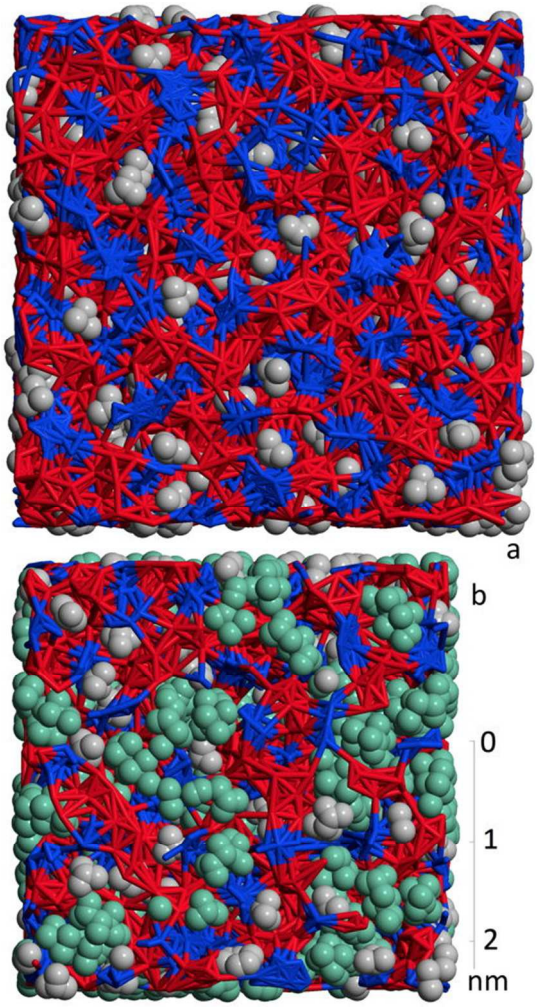

FIG 10. Selected snapshots of simulation runs in the systems [C_2mim][Ntf_2] and binary mixture of [C_2mim][Ntf_2] with 3AP.

Conclusions

The study of viscosity minima in mixtures of ILs and MSs with similar viscosity allowed us to establish a link between the structure and hydrogen-bonding capabilities of most of the different ILs and MSs and the resulting drops in the viscosity of the mixtures. The observed minima are a consequence of changes in interactions and structure between the mixtures and the pure components and should not be correlated exclusively to changes in the cohesive energy that occur in the mixing process.

Due to the inadequacy of the adopted force field to model the intramolecular interactions in 2AE it was not possible to compare the system containing this MS with the other three systems —only the fact that the cohesive energy of the [C_2mim][DCA] mixture is quasi-ideal relative to the two pure components seems to corroborate the larger viscosity drops found for the mixtures involving this MS.

In the case of the systems involving 3AP, the order of relative viscosity drops, δ ln(η/mPa.s), (for equimolar mixtures at the crossover temperature or at 298 K), given by [C_2mim][Ntf_2] <

Physical Chemistry Chemical Physics Accepted Manuscript

$[C_4mim][DCA] < [C_2mim][DCA]$, can be explained both in terms of greater H-bond losses for the $[C_4mim][DCA]$ and $[C_2mim][DCA]$ systems supplemented by a particularly severe de-structuration of the polar network in the case of $[C_2mim][DCA]$. The extremely resilient and interconnected polar network of $[C_2mim][Ntf_2]$ is a consequence of the presence of the larger and more flexible $[Ntf_2]^-$anion.

Acknowledgements

Financial support provided by Fundação para a Ciência eTecnologia (FCT) through projects FCT-ANR/CTM-NAN/0135/2012, PTDC/CTM-NAN/121274/2010, PEst-OE/EQB/LA0004/2013 and UID/QUI/00100/2013. K.S. acknowledges postdoctoral grant SFRH/BPD/94291/2013. J.M.S.S.E. acknowledges FCT for a contract under 2012 FCT Investigator.

References

1 Marsh, K. N.; Boxall, J. A.; Lichtenthaler, R. Room Temperature Ionic Liquids and Their Mixtures—A Review. *Fluid Phase Equilib.* **2004**, *219*, 93–98.
2 Wilkes, J. S. Properties of Ionic Liquid Solvents for Catalysis. *J. Mol. Catal. A: Chem.* **2004**, *214*, 11–17.
3 Seddon, K. R.; Stark, A. S.; Torres, M.-J. Viscosity and Density of 1-alkyl-3-methylimidazolium Ionic Liquids, ed. R. D. Rogers and K. R. Seddon, Ionic Liquids III: Fundamentals, Progress, Challenges, and Opportunities, ACS Symposiom Series 901, Washington DC, **2004**.
4 Ngai, K. L.; Capaccioli, S.; Paluch, M.; Prevosto, D. Temperature Dependence of the Structural Relaxation Time in Equilibrium below the Nominal T_g: Results from Freestanding Polymer Films. *J. Phys. Chem. B* **2014**, *118*, 5608–5614.
5 Mauro, J. C.; Yue, Y.; Ellison, A. J.; Gupta, P. K.; Allan, D. C. Viscosity of Glass-Forming Liquids. *PNAS* **2009**, *106*, 19780–19784.
6 Trivedi, S.; Pandey, S. Interactions within a [Ionic Liquid + Poly(ethylene glycol)] Mixture Revealed by Temperature-Dependent Synergistic Dynamic Viscosity and Probe-Reported Microviscosity. *J. Phys. Chem. B* **2011**, *115*, 7405–7416.
7 Tariq, M.; Altamash, T.; Salavera, D.; Coronas, A.; Rebelo, L. P. N.; Canongia Lopes, J. N. Viscosity Mixing Rules for Binary Systems Containing One Ionic Liquid. *ChemPhysChem* **2013**, *14*, 1956–1968.
8 Pádua, A. A. H.; Costa Gomes, M. F.; Canongia Lopes, J. N. A. Molecular Solutes in Ionic Liquids: A Structural Perspective. *Acc. Chem. Res.* **2007**, *40*, 1087–1096.
9 Silva, C. F. P.; Duarte, M. L. T. S.; Fausto, R. A Concerted SCF-MO Ab Initio and Vibrational Spectroscopic Study of the Conformational Isomerism in 2-aminoethanol. *Journal of Molecular Structure* **1999**,*482–483*, 591–599.
10 Cacela, C.; Duarte, M. L. T. S.; Fausto, R. Structural and Vibrational Characterisation of 3-amino-1-propanol a Concerted SCF-MO Ab Initio, Raman and Infrared (Matrix Isolation and Liquid Phase) Spectroscopy Study. *Spectrochimica Acta Part A* **2000**, *56*, 1051–1064.
11 Angell, C. A. Formation of Glasses from Liquids and Biopolymers. *Science* **1995**, *267*, 1924–1935.

Physical Chemistry Chemical Physics Accepted Manuscript

12 Grunberg, L.; Nissan, A. H. Mixture Law for Viscosity. *Nature* **1949**, *164*, 799–800.

13 Tariq, M.; Carvalho, P. J.; Coutinho, J. A. P.; Marrucho, I. M.; Canongia Lopes, J. N.; Rebelo, L. P. N. Viscosity of (C2–C14) 1-alkyl-3-methylimidazolium bis(trifluoromethylsulfonyl)amide Ionic Liquids in an Extended Temperature Range. *Fluid Phase Equilib.* **2011**, *301*, 22–32.

14 Paredes, X.; Fandiño, O.; Comuñas, M. J. P.; Pensado, A. S.; Fernández, J. Study of the Effects of Pressure on the Viscosity and Density of diisodecyl phthalate. *J. Chem. Thermodyn.* **2009**, *41*, 1007–1015.

15 Canongia Lopes, J. N.; Deschamps, J.; Pádua, A. A. H. Modeling Ionic Liquids Using a Systematic All-Atom Force Field. *J. Phys. Chem. B* **2004**, *108*, 2038−2047.

16 Canongia Lopes, J. N.; Pádua, A. A. H. Molecular Force Field for Ionic Liquids Composed of Triflate or Bistriflylimide Anions. *J. Phys. Chem. B* **2004**, *108*, 16893–16898.

17 Canongia Lopes, J. N.; Pádua, A. A. H. Molecular Force Field for Ionic Liquids III: Imidazolium, Pyridinium, and Phosphonium Cations; Chloride, Bromide, and Dicyanamide Anions. *J. Phys. Chem. B* **2006**, *110*, 19586–19592.

18 Jorgensen, W. L.; Maxwell, D. S.; Tirado-Rives, J. Development and Testing of the OPLS All-Atom Force Field on Conformational Energetics and Properties of Organic Liquids. *J. Am. Chem. Soc.* **1996**, *118*, 11225–11236.

19 Smith, W.; Forester, T. R. *The DL_POLY Package of Molecular Simulation Routines (v.2.2)*; The Council for The Central Laboratory of Research Councils; Daresbury Laboratory: Warrington, U.K., **2006**.

20 Leal, J. P.; Esperança, J. M. S. S. Minas da Piedade, M. E.; Canongia Lopes, J. N.; Rebelo, L. P. N.; Seddon, K. R. The Nature of Ionic Liquids in the Gas Phase. *J. Phys. Chem. A* **2007**, *111*, 6176–6182.

21 Santos, L. M. N. B. F.; Canongia Lopes, J. N.; Coutinho, J. A. P.; Esperança, J. M. S. S.; Gomes, L. R.; Marrucho, I. M.; Rebelo, L. P. N. Ionic Liquids: First Direct Determination of their Cohesive Energy. *J. Am. Chem. Soc.* **2007**, *129*, 284–285.

22 Schreiner, C.; Zugmann, S.; Hartl, R.; Gores, H. J. Fractional Walden Rule for Ionic Liquids: Examples from Recent Measurements and a Critique of the So-Called Ideal KCl Line for the Walden Plot.*J. Chem. Eng. Data* **2010**, *55*, 1784–1788.

23 Fletcher, S. I.; Sillars, F. B.; Hudson, N. E.; Hall, P. J.Physical Properties of Selected Ionic Liquids for Use as Electrolytes and Other Industrial Applications.*J. Chem. Eng. Data* **2010**, *55*, 778–782.

24 Freire, M. G.; Teles, A. R. R.; Rocha, M. A. A.; Schroder, B.; Neves, C. M. S. S.; Carvalho, P. J.; Evtuguin, D. V.; Santos, L. M. N. B. F.; Coutinho, J. A. P. Thermophysical Characterization of Ionic Liquids Able To Dissolve Biomass.*J. Chem. Eng. Data* **2011**, *56*, 4813–4822.

25 Carvalho, P. J.; Regueira, T.; Santos, L. M. N. B. F.; Fernandez, J.; Coutinho, J. A. P.Effect of Water on the Viscosities and Densities of 1-Butyl-3-methylimidazolium Dicyanamide and 1-Butyl-3-methylimidazolium Tricyanomethane at Atmospheric Pressure.*J. Chem. Eng. Data* **2010**, *55*, 645–652.

26 Shiflett, M. B.; Elliott, B. A.; Yokozeki, A. Phase Behavior of Vinyl Fluoride in Room-Temperature Ionic Liquids [emim][Tf_2N], [bmim][$N(CN)_2$], [bmpy][BF_4], [bmim][HFPS] and [omim][TFES].*Fluid Phase Equilib.* **2012**, *316*, 147–155.

Physical Chemistry Chemical Physics Accepted Manuscript

27 Yusoff, R.; Aroua, M. K.; Shamiri, A.; Ahmady, A.; Jusoh, N. S.; Asmuni, N. F.; Bong, L. C.; Thee, S. H.Density and Viscosity of Aqueous Mixtures of *N*-Methyldiethanolamines (MDEA) and Ionic Liquids.*J. Chem. Eng. Data* **2013**, *58*, 240–247.

28 Sanchez, L. G.; Espel, J. R.; Onink, F.; Meindersma, G. W.; De Haan, A. B. Density, Viscosity, and Surface Tension of Synthesis Grade Imidazolium, Pyridinium, and Pyrrolidinium Based Room Temperature Ionic Liquids.*J. Chem. Eng. Data* **2009**,*54*, 2803–2812.

29 Fendt, S.; Padmanabhan, S.; Blanch, H. W.; Prausnitz, J. M. Viscosities of Acetate or Chloride-Based Ionic Liquids and Some of Their Mixtures with Water or Other Common Solvents.*J. Chem. Eng. Data* **2011**, *56*, 31–34.

30 McHale, G.; Hardacre, C.; Ge, R.; Doy, N.; Allen, R. W. K.; MacInnes, J. M.; Brown, M. R.; Newton, M. I. Density−Viscosity Product of Small-Volume Ionic Liquid Samples Using Quartz Crystal Impedance Analysis.*Anal. Chem.* **2008**, *80*, 5806–5811.

31 Ahosseini, A.; Scurto, A. M. Viscosity of Imidazolium-Based Ionic Liquids at Elevated Pressures: Cation and Anion Effects.*Int. J. Thermophys.* **2008**, *29*, 1222–1243.

32 Beigi, A. A. M.; Abdouss, M.; Yousefi, M.; Pourmortazavi, S. M.; Vahid, A. Investigation on Physical and Electrochemical Properties of Three Imidazolium Based Ionic Liquids (1-hexyl-3-methylimidazolium tetrafluoroborate, 1-ethyl-3-methylimidazolium bis(trifluoromethylsulfonyl) imide and 1-butyl-3-methylimidazolium methylsulfate).*J. Mol. Liq.* **2013**, *177*, 361–368.

33 Jacquemin, J.; Husson, P.; Padua, A. A. H.; Majer, V. Density and Viscosity of Several Pure and Water-Saturated Ionic Liquids.*Green Chem.* **2006**, *8*, 172–180.

34 Tokuda, H.; Tsuzuki, S.; Susan, M. A. B. H.; Hayamizu, K.; Watanabe, M. How Ionic Are Room-Temperature Ionic Liquids? An Indicator of the Physicochemical Properties.*J. Phys. Chem. B* **2006**, *110*, 19593–19600.

35 Crosthwaite, J. M.; Muldoon, M. J.; Dixon, J. K.; Anderson, J. L.; Brennecke, J. F. Phase Transition and Decomposition Temperatures, Heat Capacities and Viscosities of Pyridinium Ionic Liquids. *J. Chem. Thermodyn.* **2005**, *37*, 559–568.

36 Tokuda, H.; Hayamizu, K.; Ishii, K.; Susan, M. A. B. H.; Watanabe, M. Physicochemical Properties and Structures of Room Temperature Ionic Liquids. 2. Variation of Alkyl Chain Length in Imidazolium Cation.*J. Phys. Chem. B* **2005**, *109*, 6103–6110.

37 Yao, ; Zhang, S.; Wang, J.; Zhou, Q.; Dong, H.; Zhang, X. Densities and Viscosities of the Binary Mixtures of 1-Ethyl-3-methylimidazolium Bis(trifluoromethylsulfonyl)imide with *N*-Methyl-2-pyrrolidone or Ethanol at *T* = (293.15 to 323.15) K.*J. Chem. Eng. Data* **2012**, *57*, 875–881.

38 Camper, D.; Becker, C.; Koval, C.; Noble, R. Diffusion and Solubility Measurements in Room Temperature Ionic Liquids.*Ind. Eng. Chem. Res.* **2006**, *45*, 445–450.

39 Islam, M. N.; Islam, M. M.; Yeasmin, M. N.Viscosity of Aqueous Solutions of 2-methoxyethanol, 2-ethoxyethanol, and ethanolamine. *J. Chem. Thermodyn.* **2004**, *36*, 889–893.

40 Arachchige, U. S. P. R.; Aryal, N.; Eimer, D. A.; Melaaen, M. C. Viscosities of Pure and Aqueous Solutions of Monoethanolamine (MEA), Diethanolamine (DEA) and N-Methyldiethanolamine (MDEA).*Ann. T. Nord. Rheol. Soc.* **2013**, *21*, 299–306.

Physical Chemistry Chemical Physics Accepted Manuscript

41 Li, M. H.; Lie, Y. C. Densities and Viscosities of Solutions of Monoethanolamine + N-methyldiethanolamine + Water and Monoethanolamine + 2-Amino-2-methyl-1-propanol + Water.*J. Chem. Eng. Data*. **1994**, *39*, 444–447.

42 Mandal, B. P.; Kundu, M.; Bandyopadhyay, S. S. Density and Viscosity of Aqueous Solutions of (*N*-Methyldiethanolamine + Monoethanolamine), (*N*-Methyldiethanolamine + Diethanolamine), (2-Amino-2-methyl-1-propanol + Monoethanolamine), and (2-Amino-2-methyl-1-propanol + Diethanolamine).*J. Chem. Eng. Data.* **2003**, *48*, 703–707.

43 DiGuilio, R. M.; Lee, R.-J.; Schaeffer, S. T.; Brasher, L. L.; Teja, A. S. Densities and Viscosities of the Ethanolamines. *J. Chem. Eng. Data.* **1992**,*37*, 239–242.

44 Kermanpour, F.; Niakan, H. Z. Measurement and Modeling the Excess Molar Properties of Binary Mixtures of {[C_6mim][BF_4] + 3-amino-1-propanol} and {[C_6mim][BF_4] + isobutanol}: Application of Prigogine–Flory–Patterson Theory. *J. Chem. Thermodyn.* **2012**, *48*, 129–139.

45 Omrani, A.; Rostami, A. A.; Mokhtary, M. Densities and Volumetric Properties of 1,4-dioxane with Ethanol, 3-Methyl-1-butanol, 3-Amino-1-propanol and 2-Propanol Binary Mixtures at Various Temperatures. *J. Mol. Liq.* **2010**, *157*, 18–24.

46 Acree Jr., W.; Chickos, J. S. Phase Transition Enthalpy Measurements of Organic and Organometallic Compounds. Sublimation, Vaporization and Fusion Enthalpies from 1880 to 2010. *J. Phys. Chem. Ref. Data* **2010**, *39*, 043101-1–043101-942.

47 Yaws, C. L. *Thermophysical Properties of Chemicals and Hydrocarbons*, Elsevier, 2009.

48 Esperança, J. M. S. S.; Canongia Lopes, J. N.; Tariq, M.; Santos, L. M. N. B. F.; Magee, J. W.; Rebelo, L. P. N. Volatility of Aprotic Ionic Liquids — A Review. *J. Chem. Eng. Data* **2010**, *55*, 3–12.

49 Shimizu, K.; Tariq, M.; Costa Gomes; M. F.; Rebelo, L. P. N.; Canongia Lopes, J. N. Assessing the Dispersive and Electrostatic Components of the Cohesive Energy of Ionic Liquids using Molecular Dynamics Simulations and Molar Refraction Data. . *J. Phys. Chem. B* **2010**, *114*, 5831–5834.

50 Kelkar, M. S.; Maginn, E. J. Effect of Temperature and Water Content on the Shear Viscosity of the Ionic Liquid 1-Ethyl-3-methylimidazolium Bis(trifluoromethanesulfonyl)-imide as Studied by Atomistic Simulations. *J. Phys. Chem. B* **2007**, *111*, 4867–4876.

51 Köddermann, T.; Paschek, D.; Ludwig, R. Molecular Dynamic Simulations of Ionic Liquids: A Reliable Description of Structure, Thermodynamics and Dynamics. *ChemPhysChem.* **2007**, *8*, 2464–2470.

52 Bica, K.; Deetlefs, M.; Schröder, C.; Seddon, K. R. Polarisabilities of Alkylimidazolium Ionic Liquids. *Phys. Chem. Chem. Phys.* **2013**,*15*, 2703–2711.

53 Neves, C. M. S. S.; Kurnia, K. A.; Coutinho, J. A. P.; Marrucho, I. M.; Canongia Lopes, J. N.; Freire, M. G.; Rebelo, L. P. N. Systematic Study of the Thermophysical Properties of Imidazolium-Based Ionic Liquids with Cyano-Functionalized Anions. *J. Phys. Chem. B* **2013**, *117*, 10271−10283.

54 Tariq, M.; Forte, P. A. S.; Costa Gomes, M. F.; Canongia Lopes, J. N.; Rebelo, L. P. N. Densities and Refractive Indices of Imidazolium- and Phosphonium-based Ionic Liquids: Effect of Temperature, Alkyl Chain Length, and Anion. *J. Chem. Thermodyn.* **2009**, *41*, 790–798.

Physical Chemistry Chemical Physics Accepted Manuscript

55 Verevkin, S. P.; Emel'yanenko, V. N.; Zaitzau, D. H.; Heintz, A.; Muzny, C. D.; Frenkel, M. Thermochemistry of Imidazolium-based Ionic Liquids: Experiment and First-Principle Calculations. Phys. Chem. Chem. Phys. **2010**, *12*, 14994–15000.

56 Thomsen, D. L.; Axson, J. L.; Schrøder, S. D.; Lane, J. R.; Vaida, V.; Kjaergaard, H. G. Intramolecular Interactions in 2-Aminoethanol and 3-Aminopropanol. *J. Phys. Chem. A* **2013**, *117*, 10260–10273.

57 Gubskaya, A. V.; Kusalik, P. G. Molecular Dynamics Simulation Study of Ethylene Glycol, Ethylenediamine, and 2-Aminoethanol. 1. The Local Structure in Pure Liquids. *J. Phys. Chem. A* **2004**, *108*, 7151–7164.

58 Pádua, A. A. H.; Canongia Lopes, J. N. Nanostructural Organization in Ionic Liquids. *J. Phys. Chem. B* **2006**, *110*, 3330−3335.

59 Shimizu, K.; Bernardes, C. E. S.; Canongia Lopes, J. N. Structure and Aggregation in the 1-Alkyl-3-MethylimidazoliumBis(trifluoromethylsulfonyl)imide Ionic Liquid Homologous Series. *J. Phys. Chem. B* **2014**, *118*, 567−576.

Physical Chemistry Chemical Physics Accepted Manuscript